

Directed self-assembly of monodispersed platinum nanoclusters on graphene Moiré template

Yi Pan,¹ Min Gao,¹ Li Huang,¹ Feng Liu,² and H.-J. Gao^{1,a)}

¹*Institute of Physics, Chinese Academy of Sciences, Beijing 100190, People's Republic of China*

²*Department of Materials Science and Engineering, University of Utah, Salt Lake City, Utah 84112, USA*

(Received 9 July 2009; accepted 16 August 2009; published online 3 September 2009)

Monodispersed crystalline platinum nanoclusters (NCs) have been grown on a template of graphene Moiré pattern formed on Ru(0001). The Pt NCs are directed to nucleate at a unique site in the Moiré unit cell, and grow in a layer-by-layer mode up to 4-atomic-layer height without coalescence at room temperature. The size of Pt NCs can be controlled by tuning the coverage. This system may find application in the study of Pt nanocatalyst, and the graphene Moiré pattern may be generally applied as template to direct self-assembled growth of metallic or nonmetallic NCs. © 2009 American Institute of Physics. [DOI: 10.1063/1.3223781]

When the size shrunk to nanometer dimension, metal clusters exhibit quantum size effect¹ and unusual chemical reactivity,² which may find applications in electronics and catalysis industries. Thus many physical and chemical routes to produce metal nanoclusters (NCs) have been developed in the past decades, such as ion sputtering, vapor aggregation in cold inert gas and decomposition of an organometallic complex.^{3,4} However, the problem of controlling the size and arrangement of metal NCs remains to be fully solved. One effective solution of utilizing thin film template or patterned substrate have been developed recently.⁵⁻⁹ By directly depositing metal atoms on the template of orderly rippled thin film that grown on metal crystal substrate, metal clusters with precisely controlled size and arrangement can be obtained. One thin film template is the nanomesh of corrugated boron-nitride layer on Ru(0001) or Rh(111), on which the uniform gold and cobalt NC hexagonal arrays have been fabricated.^{5,6} Another thin film template is the graphene Moiré pattern on Ir(111), on which the highly ordered uniform iridium NC hexagonal arrays were produced.⁷

In this letter, we report on the self-assembled growth of monodispersed platinum NCs on another thin film template, the Moiré structure of graphene on Ru(0001). Because graphene monolayer film formed on Ru(0001) surface is of good quality with highly ordered Moiré pattern in large area, it provides an excellent template. Moreover, since carbon material is commonly used as support for noble metal catalyst, such as Pt/activated carbon catalysts that had been employed in many selective hydrogenation reactions,¹⁰ graphene Moiré pattern template may serve as a candidate system for the study of platinum nanocatalyst.

Our experiments were carried out in a UHV system with base pressure lower than 1×10^{-10} mbar. The graphene Moiré template was grown on Ru surface by carbon segregation, which was presented in detail elsewhere.^{11,12} Platinum was deposited onto the template from a platinum rod (purity of 99.99%) mounted on the evaporator, with the deposition rate maintained at 0.01 ML/min (1 ML = 1.6×10^{15} atoms/cm²) by monitoring the ion current flux of the platinum vapor beam. The Pt coverage had been calibrated by growing submonolayer film on pristine Ru substrate.

Samples were checked with Auger electron spectroscopy to rule out contaminants and then studied with room temperature (RT) scanning tunneling microscope (STM) at constant current mode.

At a low coverage of 0.05 ML, the Pt NCs dispersedly nucleate on the template, as shown in the STM topographic image in Fig. 1(a). The blue spots arranged in a hexagonal array in the image are the Moiré pattern of graphene on Ru(0001) substrate. The monodispersed Pt NCs, which appear as colored protrusions, only exist at certain sites of the template where the adjacent three Moiré spots form a down-pointing triangle as illustrated in Fig. 1(a). This implies that the template directs the nucleation of NCs at a unique site in the Moiré unit cells. To present this fact more clearly, rectangular area in Fig. 1(a) is zoomed in and shown in Fig. 1(b) with the unit cells of the Moiré pattern marked by rhombuses. There are three distinctive regions labeled α , β , and γ inside a rhombus, among which the Pt NC locates in the β region.

The vertical height of NCs is encoded in different colors, as indicated by the color bar in Fig. 1(b). The Pt NCs display three typical heights as implied by the colors (cyan, red, and yellow). Figure 1(c) shows a height profile curve over three NCs along the arrowed line in Fig. 1(a). It reveals that the typical NC heights are 1.27 nm, 0.5 nm and 0.88 nm, which

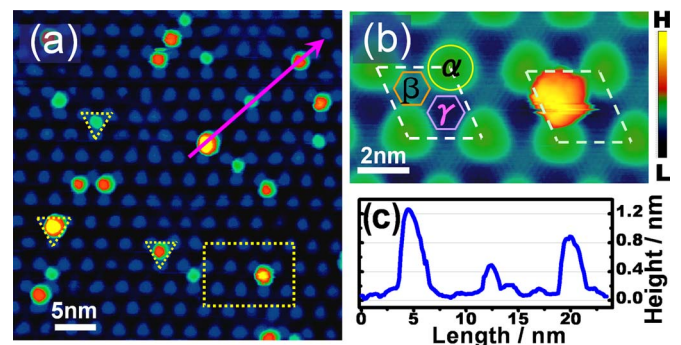


FIG. 1. (Color online) (a) STM topographic image of Pt NCs on graphene/Ru(0001) Moiré template. The height is indicated as in the color bar. (b) Zoom in the rectangular in (a). The rhombuses show Moiré pattern unit cells, with the three distinctive regions labeled by α , β , and γ . The Pt NC locates in the β region. (c) Line profile of three clusters along the purple arrow in (a), showing their typical heights are 1.27, 0.5, and 0.88 nm.

^{a)}Electronic mail: hjgao@iphy.ac.cn.

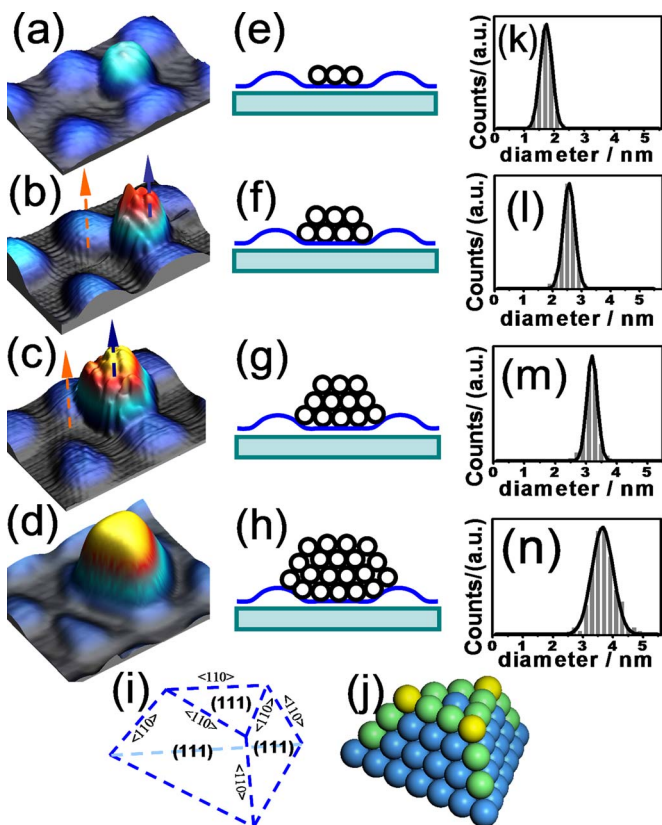


FIG. 2. (Color online) [(a)–(d)] 3D STM topographic images, [(e)–(h)] sketches and [(k)–(n)] diameter distributions of Pt NCs of 1, 2, 3, and 4-atomic-layer height. (i) Structure model of 4-atomic-layer Pt NC, showing the framework of frustum of triangular pyramid with fcc (111) facets and fcc $\langle 110 \rangle$ edges. (j) Ball model of 4-atomic-layer Pt NC, showing the atoms with coordination number 5, 7, and 9 (blue, green, and yellow) on the facets, edges and corners.

correspond to Pt NCs consisting of three, one, and two atomic layers, respectively, given that their height difference ($\Delta H \approx 0.38$ nm) equals to the apparent step height of Pt(111) surface. At even higher Pt coverage, we also observed Pt NC of 1.65 nm height, containing four atomic layers. These results indicate that after the NCs nucleate inside a Moiré unit cell, they grow in a layer-by-layer mode increasing their height without coalescence at RT.

To further resolve the morphology of NCs of different heights, a series of three-dimensional (3D) STM topographic images are displayed in Figs. 2(a)–2(d). Their respective atomic models are sketched as in Figs. 2(e)–2(h). The monolayer NC [Fig. 2(a)] is relatively small, showing blurred edge and rough surface with low resolution. They are unstable at RT and could easily be swept away by the STM tip during scanning. The 2-layer [Fig. 2(b)] and 3-layer [Fig. 2(c)] NCs show sharp edges but rough surfaces with high resolution. Although their top surfaces are not smooth, the height protrusions on the top arrange in the same orientation as the carbon atoms in the graphene template, as indicated by the parallel arrows in Figs. 2(b) and 2(c). The 4-layer NC [Fig. 2(d)] is most distinctive as it displays highly crystallized structure with smooth top and facets. According to the 3D STM image, a structure model with the shape of a frustum of triangular pyramid is constructed in Fig. 2(i). The top surface is the fcc (111) facet, which is consistent with the substrate hcp (0001) surface, although a lattice mismatch exists at the interface. The side facets are all fcc (111) planes in accor-

dance with the side slope angles in the 3D STM image. The edges are in fcc $\langle 110 \rangle$ direction, in line with the substrate hcp $\langle 1000 \rangle$ direction. A ball model of the 4-layer cluster is shown in Fig. 2(j), in which the low-coordination-number atoms on the edges and corners, with respective coordination number of 7 and 5, are displayed in green and yellow. These edge and corner atoms may play an important role in catalytic reaction.⁴

In addition, size distribution of different heights of NCs has been carefully measured and calibrated through statistical analysis of dozens of STM images. The statistics results of NC diameters are shown in Figs. 2(k)–2(n) as histograms with fitted curves. It indicates that the NCs with different heights have similar diameter distribution function, which is quite narrow with full width at half maximum less than 1 nm. Peak positions of the curves suggest that the most favorable diameters are 1.7, 2.5, 3.2, and 3.7 nm, for 1, 2, 3, and 4-layer NCs, respectively.

The directed nucleation of Pt NCs at a preferred region [β region as in Fig. 1(b)] in the Moiré unit cell is believed to be caused by the preferential Pt atom adsorption at these unique sites. On the polar FeO film, the preferential adsorption is attributed to the large vertical surface dipole associated with the preferred domain in the Moiré cell.⁸ On the nonpolar graphene film on Ir(111), Feibelman *et al.*¹³ found that the preferential adsorption was due to the local rehybridization of the C–C bonds from sp^2 to sp^3 in the adsorption region, which could be applied to our case of graphene on Ru(0001). The carbon atoms in the β region [Fig. 1(b)] can be classified as C_{top} and C_{hollow} according to their positions with respect to the substrate. C_{top} is lower moving toward substrate due to the interaction with Ru atom below, but C_{hollow} is higher without such interaction. This gives rise to a local structural distortion, which has been shown by both experiment¹² and first principle calculation.¹⁴ As a result, the C–C bond rehybridization occurs by breaking the C–C π bond to form a $C_{\text{top}}\text{–Ru}$ σ bonds and an upward dangling bond on C_{hollow} . Then, the Pt atoms could be easily trapped in the β region by interacting with the dangling bond on C_{hollow} . In contrast, there is no such structural distortion in the α and γ regions and all the C atoms there remain π -bonded with on dangling bonds to trap Pt atoms.

Since upon nucleation the Pt NCs grow in a layer-by-layer mode to increase their height with a concomitant slow increase in diameter, but without coalescence at RT, we are able to control their size to some extent by deposition. A series of STM images with Pt coverage of 0.02, 0.05, 0.12, 0.24, and 0.36 ML are shown in Figs. 3(a)–3(e). With the increasing coverage, more NCs nucleate one each inside a Moiré unit cell while at the same time the existing NCs grow slowly their size. All the NCs remain separated throughout and big islands resulted from coalescence or coarsening could seldom be seen. Also, NCs with a given height (1, 2, 3, or 4-atomic-layer) continue to remain monodispersed with a narrow size (diameter) distribution. This indicates the self-limited diameter growth, i.e., the NC at a given height (let us say 2-layer) would not grow its diameter too much before growing its height (to 3-layer). This is because the Moiré pattern provides certain confinement effect to limit the NC growing laterally, so that there remains one NC per Moiré unit cell without coalescence. Such self-limiting growth in NC diameter apparently helps to improve the NC size uni-

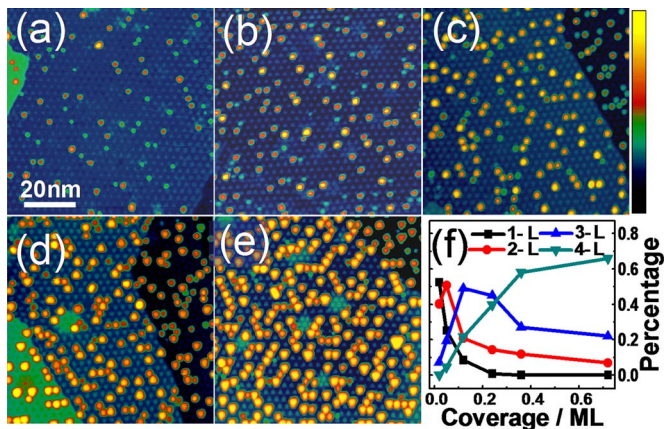


FIG. 3. (Color online) [(a)–(e)] STM topographic images with Pt coverage of 0.02, 0.05, 0.12, 0.24, and 0.36 ML. The height is displayed as in the color bar. All the images are taken at $V_b = -1.5$ V, $I_t = 1.0$ nA, and of the same size as indicated by the bar in (a). (f) The percentages of the four types (1, 2, 3, and 4-atomic-layer) of clusters with the increase in Pt coverage.

formity. It also helps to increase NC number density (nucleation) with increasing coverage. The varying percentages of each type of NCs were shown in Fig. 3(f). The monolayer NCs are dominating at low coverage of 0.02 ML, and the 2-layer NCs reach the maximum percentage at 0.05 ML, and then the 3-layer and 4-layer NCs become prominent successively with the increasing Pt coverage. Under even higher coverage (>1 ML), the NCs start to coalesce into islands and eventually into film. These results suggest that the size and shape of the Pt NCs could be controlled to a good extent by carefully tuning the coverage.

We note that the density of self-assembled Pt NCs on graphene/Ru(0001) as observed here is lower than that of Ir NCs on graphene/Ir(111).⁷ We attribute this difference to the different diffusion coefficient (D) in the two systems. The NC nucleation rate and hence the number density up to a certain coverage depends on D at a given deposition rate. We deduce that D_{Ir} is lower than D_{Pt} because the bond enthalpy of Ir–C (632 ± 4 kJ/mol) is higher than Pt–C (598 ± 5.9 kJ/mol).¹⁵ The larger D_{Pt} means smaller nucleation rate of Pt NCs than that of Ir NCs, yielding a lower number density of NC. The density of metal NCs would

affect the chemical reaction rate when these systems are used to study the model catalyst systems.¹⁶

In conclusion, monodispersed Pt NCs with the diameter of 2–3 nm have been grown by depositing platinum on the Moiré template of graphene film on Ru(0001) surface. The Pt NCs are directed by the template to nucleate preferentially at a unique region in the Moiré unit cell, which leads to the formation of self-assembled Pt NC array. With increasing deposition, the NCs grow in a layer-by-layer mode to increase their height and exhibit a self-limited growth mode in diameter without coalescence. The size of Pt NCs could be controlled to a certain extent by tuning the coverage. We suggest that the Moiré template of graphene/Ru(0001) could potentially be extended to the fabrication NCs of many other metallic or nonmetallic materials, with potential application in metal nanocatalysis.

The authors gratefully acknowledge financial support from NSF of China, National “863” and “973” projects of China and DOE of United States of America.

- ¹W. P. Halperin, *Rev. Mod. Phys.* **58**, 533 (1986).
- ²H.-G. Boyen, G. Kastle, F. Weigl, B. Koslowski, C. Dietrich, P. Ziemann, J. P. Spatz, S. Riethmuller, C. Hartmann, M. Moller, G. Schmid, M. G. Garnier, and P. Oelhafen, *Science* **297**, 1533 (2002).
- ³W. A. de Heer, *Rev. Mod. Phys.* **65**, 611 (1993).
- ⁴J. Chen, B. Lim, E. P. Lee, and Y. Xia, *Nanotoday* **4**, 81 (2009).
- ⁵A. Goriachko, Y. He, M. Knapp, H. Over, M. Corso, T. Brugger, S. Berner, J. Osterwalder, and T. Greber, *Langmuir* **23**, 2928 (2007).
- ⁶I. Brihuega, C. H. Michaelis, J. Zhang, S. Bose, V. Sessi, J. Honolka, M. A. Schneider, A. Enders, and K. Kern, *Surf. Sci.* **602**, L95 (2008).
- ⁷A. T. N’Diaye, S. Bleikamp, P. J. Feibelman, and T. Michely, *Phys. Rev. Lett.* **97**, 215501 (2006).
- ⁸N. Nilius, E. D. L. Rienks, H.-P. Rust, and H.-J. Freund, *Phys. Rev. Lett.* **95**, 066101 (2005).
- ⁹H. Hu, H. J. Gao, F. Liu, *Phys. Rev. Lett.* **101**, 216102 (2008).
- ¹⁰F. Rodriguez-Reinos, *Carbon* **36**, 159 (1998).
- ¹¹Y. Pan, D. X. Shi, and H.-J. Gao, *Chin. Phys. Lett.* **16**, 3151 (2007).
- ¹²Y. Pan, H. Zhang, D. X. Shi, J. Sun, S. X. Du, F. Liu, and H.-J. Gao, *Adv. Mater.* **21**, 2777 (2009).
- ¹³P. J. Feibelman, *Phys. Rev. B* **77**, 165419 (2008).
- ¹⁴B. Wang, M.-L. Bocquet, S. Marchini, S. Gunther, and J. Wintterlinbc, *Phys. Chem. Chem. Phys.* **10**, 3530 (2008).
- ¹⁵J. A. Kerr, *CRC Handbook of Chemistry and Physics 1999–2000: A Ready-Reference Book of Chemical and Physical Data*, 81st ed. (CRC, Boca Raton, Florida, 2000).
- ¹⁶J. Libuda and H.-J. Freund, *Surf. Sci. Rep.* **57**, 157 (2005).